SURFACE ACOUSTIC WAVE GRATINGS OF FINITE WIDTH

by

André Antoine Merab
B.S., Massachusetts Institute of Technology
(1975)

SUBMITTED IN PARTIAL FULFILLMENT OF THE
REQUIREMENTS FOR THE DEGREE OF
MASTER OF SCIENCE
at the
MASSACHUSETTS INSTITUTE OF TECHNOLOGY
May, 1979

Signature of Author: Signature redacted
Department of Electrical Engineering and Computer Science, May 18, 1979

Certified by: Signature redacted
Thesis Supervisor

Accepted by: Signature redacted
Chairman, Departmental Committee

SURFACE ACOUSTIC WAVE GRATINGS OF FINITE WIDTH

by

André Antoine Merab

Submitted to the Department of Electrical Engineering and Computer Science on May 18, 1979, in partial fulfillment of the requirements for the Degree of Master of Science.

ABSTRACT

Surface Acoustic Wave gratings of finite width support a finite number of transverse modes. A theory of the excitation of these modes, based on a coupled-mode formalism, is developed and checked against the experimental results of Mason et al. on shorted and open metal-strip gratings. The theory does not, as yet, explain the observed mode structure in the shorted strip grating (isotropy and excitation by a uniform input apodization over the width of the grating were assumed). It is, however, in excellent agreement with the experimental observations on the open-strip grating for which a study of the dispersion relation, of the mode structure and its frequency dependence, and of the effect of apodization on the selective excitation of grating modes is presented.

Thesis Supervisor: Hermann A. Haus

Title: Elihu Thomson Professor of Electrical Engineering

ACKNOWLEDGEMENTS

I wish to express my thanks and my sincere appreciation to Professor Hermann Haus for his invaluable guidance during the preparation of this work. Thanks are also due the Mathlab Group, MIT Laboratory for Computer Science, for the use of Macsyma, and to Mrs. Delphine Radcliffe for typing the thesis so nicely.

Thanks to my parents for their love and constant encouragement.

TABLE OF CONTENTS

I. INTRODUCTION

1.1 Surface Acoustic Waves

Surface Acoustic Waves (SAW), or Rayleigh Waves, are elastic waves that are confined to the surface of solids and propagate with velocity independent of frequency.[1-3] The current interest in SAW is due in large part to their relatively low velocity compared to that of electromagnetic waves. SAW are typically five orders of magnitude slower than electromagnetic waves. This fact, in conjunction with the high Q of acoustic media, makes possible the construction of delay lines with delays a hundred times that of low-loss electromagnetic waveguides. It also means that components whose size is of the order of the wavelength - i. e. most microwave components - can be realized in a volume which, in principle, could be fifteen orders of magnitude smaller than that required by their electromagnetic counterparts. SAW devices also hold a clear edge over bulk acoustic wave devices. The archetypal bulk device, the quartz resonator, becomes too fragile above 50 MHz (its resonant frequency is inversely proportional to crystal thickness). By contrast, SAW resonators are rugged (only one surface must be free). They offer high Q (10^5), low insertion loss (< 5 dB), impedance levels in the 10-1000 ohm range, and operating frequencies an order of magnitude higher than comparable bulk devices.

A SAW device is typically comprised of a piezoelectric substrate material with an optically polished surface and of transducers to convert between electrical and acoustic signals. An efficient transducer was not available until the introduction of the interdigital transducer (IDT) by White and Voltmer.[4] The properties of the IDT were immediately

exploited in the design of interdigital transversal filters.[5] This approach is not always satisfactory since the dual role of the IDT, to transduce and to determine response, leads to conflicting requirements with subsequent loss of performance. In particular, the need for radar expanders and compressors with wide bandwidth and large compression ratio stimulated the development of the devices studied in this thesis - SAW gratings - where the response is not dictated by transducers but by surface structures.

1.2 Surface Acoustic Wave Gratings

A direct analogy exists between Rayleigh wave propagation and the propagation of paraxial beams in optics.[6] High reflectivity mirrors are used in optics to build Fabry-Perot resonators. Similar SAW resonators would require strong localized reflectors of Rayleigh waves. Pending the discovery of such reflectors, grating reflectors are used. These distributed reflectors utilize the Bragg scattering from a periodic array of discontinuities to achieve very high reflectivities ($\sim$ 98%) over a narrow bandwidth with relatively low reflectivity per discontinuity (- 40 dB). A Fabry-Perot type resonator results when two strong distributed reflectors are appropriately separated to form a cavity. The idea of forming such an acoustic cavity on a piezoelectric substrate was first proposed by Ash[7] in 1970 and demonstrated experimentally by Staples[8] in 1974. Coupling into the system is effected by means of one or more standard interdigital transducers.

The development of SAW resonators has been considerable in RF systems, providing a wide range of important filtering, signal processing, and frequency control operations. Yet, a variety of second order effects stand in the way of obtaining a desirable resonance characteristic:[9]

longitudinal modes of the cavity, device loss, asymmetry of the insertion loss curves and transverse modes, all with a detrimental effect on the Q of the resonator.[10]

Transverse modes stem from the limited transverse extent of SAW transducers imposed by size restrictions and impedance requirements. Such modes are particularly troublesome since they may lead to spurious resonances close to and on the high side of the main resonance peak.[11] The recent theoretical work of Haus and Wang[12-14] has elucidated the structure of these modes and their complex frequency dependence. This thesis, based on their approach, addresses itself to the excitation of transverse grating modes in finite width SAW gratings and the effect of transducer apolization on their selective excitation.

II. TRANSVERSE GRATING MODES

2.1 Introduction

An analytical solution to SAW propagation in grating reflectors is not available. Scattering of elastic waves from obstacles is an exceedingly difficult problem, much more intricate than its electromagnetic counterpart. Cambiaggio et al.[15,16] have used the finite difference method to obtain computer solutions to the scattering of SAW from one or two metallic strips on a piezoelectric substrate, but they have been frustrated in their attempts to obtain numerical solutions when the number of strips is increased.[17] In spite of the complexity of the problem, a theoretical understanding of SAW propagation in gratings has been attained by Haus[12] through the judicious combination of the paraxial wave approximation with the coupling of modes formalism. That approach is examined in this chapter.

2.2 Paraxial Wave Equation

Surface wave propagation on a semi-infinite, isotropic solid can be completely described by a single scalar potential ψ which obeys the two-dimensional wave equation:[18]

$$\frac{\partial^2\psi}{\partial x^2} + \frac{\partial^2\psi}{\partial y^2} + k^2\psi = 0 \qquad (2\text{-}1)$$

where k is the wavenumber, and (x,y) the coordinates of the surface.

For propagation directions close to three-, four-, or six-fold axes in elastically anisotropic media, the longitudinal wavenumber is given by

$$k(\theta) = k_o (1 + \alpha\theta^2) \qquad (2\text{-}2)$$

for small θ. The anisotropic parameter α is a function of the elastic moduli when $\vec{k}$ deviates from the pure-mode axis. The wave equation (2-1) can be altered to account for the anisotropy expressed in (2-2),

$$\frac{\partial^2 \psi}{\partial x^2} + \gamma \frac{\partial^2 \psi}{\partial y^2} + k^2 \psi = 0 \tag{2-3}$$

with $\gamma = \sqrt{1-2\alpha}$.

Assuming near plane-wave behaviour and substituting a forward wave[†]

$$R = R(x,y)\, e^{-jk_o x} \tag{2-4}$$

into (2-3) yields

$$\nabla_T^2 R - 2jk \frac{\partial R}{\partial x} = 0 \tag{2-5}$$

where $\nabla_T = \hat{x} \frac{\partial}{\partial x} + \hat{y}\, \gamma \frac{\partial}{\partial y}$.

The paraxial wave equation obtains when R is a weakly varying function of x, i.e.

$$\left| \frac{\partial^2 R}{\partial x^2} \right| << \left| k^2 \frac{\partial R}{\partial x} \right| \tag{2-6}$$

Then,

$$\gamma^2 \frac{\partial^2 R}{\partial y^2} - 2jk \frac{\partial R}{\partial x} = 0 \tag{2-7}$$

The paraxial wave equation (2-7) can be used to obtain the classical results of surface wave diffraction on anisotropic substrates (parabolic approximation):

(a) Dividing equation (2-7) by γ^2, one can deduce that the

[†] In optics, the electric field $\vec{E} = \hat{x}R$, (2-1) is only approximate since $\nabla \cdot \vec{E} \neq 0$. Here it is legitimate.

profile at a distance x along the pure-mode axis is equivalent to the profile predicted in an isotropic medium ($\gamma = 1$) at a distance γx. As α approaches 0.5, the aperture profile is maintained out to large distances (autocollimated beam). For $\gamma > 1$, the far-field distribution is closer to the aperture than it is in the isotropic case, while $\gamma < 1$ indicates that the beam-spreading is slower than in the isotropic case. These results are an obvious by-product of the paraxial wave equation. This should be contrasted with the laborious proof of Cohen[19] which involves the solution of the related problem of electromagnetic diffraction in uniaxially anisotropic media. (Cohen's work is the basis for the standard work of Slobodnik and Szabo[20,21].) In the coupling of modes formalism for gratings of finite width, scaling x entails scaling the coupling constant $\varkappa$. Alternatively, one could scale y, altering the width of the grating, while keeping x and $\varkappa$ unchanged.[22]

(b) The solutions to the paraxial wave equation (2-7) are the well-known Hermite-Gaussians. This fact, an immediate consequence of equation (2-7), should be contrasted with the proof given of it by Mason and Ash.[23]

2.3 Coupling of Modes

The grating discontinuities are regarding as a small periodic perturbation of the surface. Thus, the wave propagation in the periodic medium can be treated by an exact Floquet formulation with the solution expressed as an infinite sum of space harmonics.[24] Yariv[25] has shown that the simpler coupled-mode approach is formally equivalent to the Floquet formulation near the Bragg regime since they both yield the same dispersion diagram.

The coupled-mode formalism was developed by Pierce[26,27] and

used extensively in integrated optics,[28] notably in the investigation of distributed-feedback lasers by Kogelnik and Shank.[29] It was introduced in the study of surface wave gratings of infinite width by Haus,[3] and then generalized to include diffraction effects in gratings of finite width.[12,13]

The starting point of the analysis is to couple the paraxial wave equation of a forward wave R, equation (2-7), to a similar equation for a backward wave S through a coupling $\varkappa$

$$-\frac{\partial R}{\partial x} - j\left(\delta + \frac{1}{2k_o}\frac{\partial^2}{\partial y^2}\right)R = j\varkappa S \tag{2-8}$$

$$\frac{\partial S}{\partial x} - j\left(\delta + \frac{1}{2k_o}\frac{\partial^2}{\partial y^2}\right)S = j\varkappa^* R \tag{2-9}$$

where $\delta = \frac{\omega}{v} - \frac{\pi}{\Lambda}$

Λ = grating period

k_o = axial wavenumber in the $e^{\pm jk_o x}$ dependence of R and S (removed from (2-8) and (2-9)), $k_o = \pi/\Lambda$.

The detuning parameter, δ, is a measure of frequency deviation from the Bragg condition ($\delta = 0$). When the velocity v_o under the grating is different from the velocity v outside it, detuning becomes y-dependent:

$$\delta = \begin{cases} \delta_o = \frac{\omega}{v_o} - \frac{\pi}{\Lambda}, & y < |w| \\ \delta \approx \delta_o - k_o \frac{\Delta v}{v}, & y > |w| \end{cases} \tag{2-10}$$

where the fractional velocity change $\frac{\Delta v}{v} = \frac{v - v_o}{v}$.

2.4 Frequency Dependence of $\varkappa$

It is clear from the coupled-mode equations that - if second-order

effects are neglected - the coupling constant κ is the only parameter needed to analyze the grating reflector. A detailed account of the physical basis for κ is given in Chapter III. The coupling constant is, in general, frequency dependent. Experimental studies of grooved gratings lead to an empirical result for the reflection coefficient of a groove:[31]

$$r \approx \frac{2}{3}\,\frac{h}{\lambda}\,, \qquad \frac{h}{\lambda} \ll 1 \tag{2-11}$$

where h is the groove depth and λ the wavelength. The coupling coefficient is the reflection coefficient per grating period

$$\kappa = \frac{4}{3}\,\frac{h}{\lambda^2} \tag{2-12}$$

Thus, at a detuning δ from Bragg

$$\kappa(\delta) \approx \kappa_o \frac{\lambda_o^2}{\lambda^2} \tag{2-13}$$

where κ_o is $\kappa(\delta = 0)$ and λ_o is the wavelength at Bragg. Taylor-expanding $\kappa(\delta)$

$$\kappa(\delta) = \kappa_o + \frac{2\kappa_o}{\beta_o}\delta + O(\delta^2) \tag{2-14}$$

which for small δ yields

$$\kappa(\delta) = \kappa_o\left(1 + \frac{2\delta}{\beta_o}\right) \tag{2-15}$$

a result inferred by Wang and Haus[13] from an analogy with the electromagnetic problem treated by Lee.[32] Although experimental evidence is scant, a similar result seems to hold in metal-strip reflectors (cf. Chapter III), that is $\kappa = 1/(m\lambda)$. For the coupled-mode formalism to be valid, $m \gg 1$. When $m \leqslant 1$, two things happen: (1) It is improbable that one could still obtain a reflected surface wave. (2) The

appropriate normal modes cease to be forward and backward waves with weak coupling between them, but are rather the trapped motions in individual wells, also weakly coupled.

2.5 Dispersion Relation

The coupled-mode equations can be solved for the wave amplitudes when an $e^{-\alpha x}$ dependence is assumed

$$\left[\varkappa^2 - \alpha^2 - \left(\delta_o + \frac{1}{2k_o}\frac{\partial^2}{\partial y^2}\right)^2\right]R(y) = 0 \qquad (2\text{-}16)$$

with a similar equation for S(y). Equation (2-16) has four solutions which split up into a symmetric set and an antisymmetric set. The symmetric solution is the only one of interest in what follows. Under the grating ($y < |w|$)

$$R = \left[A \cos a_1 y + B \cosh a_2 y\right] e^{-\frac{\alpha}{m}x} \qquad (2\text{-}17)$$

where

$$a_1 = p\sqrt{\sqrt{1-\alpha^2} + \delta_o}$$

$$a_2 = p\sqrt{\sqrt{1-\alpha^2} - \delta_o}$$

$$m = 1/\varkappa\lambda, \qquad p = 2\sqrt{\frac{\pi}{m}}$$

α and δ_o have been normalized with respect to $\varkappa$, and distances x and y are measured in wavelengths

The forward wave decays exponentially away from the grating ($y > |w|$) with decay constant

$$b = p\sqrt{-\delta - j\alpha}, \qquad \mathrm{Re}(b) > 0 \tag{2-18}$$

For the S wave, the decay constant is b^*.

Corresponding to the forward wave R (equation (2-17)) there exists a backward wave S,

$$S = \eta A \left(\cos a_1 y - \frac{\eta^*}{\eta}\frac{B}{A}\cosh a_2 y\right) \tag{2-19}$$

where

$$\eta = \sqrt{1-\alpha} - j\alpha, \qquad |\eta| = 1$$

$$\frac{B}{A} = \frac{a_1 \sin a_1 w - b\cos a_1 w}{a_2 \sinh a_2 w + b\cosh a_2 w}$$

(obtained by matching R, $\frac{\delta R}{\delta y}$ at y = w)

If the detuning parameter δ is real, equation (2-9) complex conjugated becomes identicial to equation (2-8) if R is identified with S^*. Thus $R = \xi S^*$. The proportionality constant ξ must have unity magnitude since $|R|^2 = |S|^2$. (In the stopband, the real time-average power flow is zero. Power flowing in via R is carried back by S.) Since $|\eta| = 1$ in equation (2-19) this imposes the condition

$$\frac{B^*}{A^*} = -\frac{\eta^*}{\eta}\frac{B}{A} \tag{2-20}$$

which leads to the dispersion relation

$$\mathrm{Re}\left[\eta \frac{a_1 \sin a_1 w - b\cos a_1 w}{a_2 \sinh a_2 w + b\cosh a_2 w}\right] = 0 \tag{2-21}$$

This is a compact form of the "determinantal equation" obtained by Haus and Wang[13] through the matching of R, S, $\frac{\delta R}{\delta y}$ and $\frac{\delta S}{\delta y}$ at a grating edge.

The forward wave outside the grating is given by:

$$R = \frac{a_1 \sin a_1 w \cosh a_2 w + a_2 \cos a_1 w \sinh a_2 w}{b \cosh a_2 w + a_2 \sinh a_2 w} e^{-b(|y| - w)} \quad (2\text{-}22)$$

It should be obvious from the preceding discussion that S can be expressed very simply as

$$S = \eta R(\alpha \rightarrow -\alpha, y) e^{-\alpha x} \quad (2\text{-}23)$$

both inside and outside the grating.

III. MODE EXCITATION

> It would be difficult to find a physical science without orthogonal functions.
>
> E. T. Bell

Grating modes can be obtained for any reflective array given its width and the appropriate coupling constant. One would like to expand arbitrary SAW profiles into a superposition of these grating modes. This requires that the grating modes be orthogonal in some way, and that in conjunction with the radiation field they satisfy completeness (which essentially means that a spatial impulse can be resolved into a sum of radiation field and grating modes). Completeness is taken for granted on physical grounds. The proof of orthogonality, however, is essential.

3.1 Orthogonality Relation

Assume two forward wave modes with transverse distributions $r_m(y)$ and $r_n(y)$ and decay rates α_m and α_n. A standard trick to find orthogonality relations involves expressions of the form $\int(R_m R_n^* - S_m S_n^*)\,dy$. These are not useful in the stopband since the modes are evanescent and do not carry net power in the x-direction. However, the coupled-mode equations admit two solutions: growing modes denoted by a (+) superscript, and decaying modes denoted by a (-) superscript. As in a metallic electromagnetic waveguide driven below cut-off, the combination of growing and decaying evanescent waves can carry net power along the guide. This suggests the manipulations to be performed on the coupled-mode equations: Write a set of coupled-equations for r_m^{+*} and

s_m^{+*} and a corresponding set for r_n^- and s_n^-. Multiply the former set by r_n^- and s_n^- respectively and the latter by r_m^{+*} and s_m^{+*}. By adding the resulting equations and integrating over the transverse direction, one obtains

$$(\alpha_n - \alpha_m) \int_a^b (r_m^{+*} r_n^- - s_m^{+*} s_n^-)dy = \frac{j}{2k_o} \left[r_n^- \frac{\partial}{\partial y} r_m^{+*} - r_m^{+*} \frac{\partial}{\partial y} r_n^- + s_n^- \frac{\partial}{\partial y} s_m^{+*} - s_m^{+*} \frac{\partial}{\partial y} s_n^- \right] \Bigg|_a^b \tag{3-1}$$

For odd modes, the limits of integration are 0 and ∞, while for even modes the limits are $-\infty$ and $+\infty$. The right-hand-side of equation (3-1) vanishes (even modes)

$$(\alpha_m - \alpha_n) \int_{-\infty}^{\infty} (r_m^{+*} r_n^- - s_m^{+*} s_n^-)\, dy = 0 \tag{3-2}$$

This is the orthogonality relation; unless $\alpha_n = \alpha_m$, $\int_{-\infty}^{\infty} (r_m^{+*} r_n^- - s_m^{+*} s_n^-)dy = 0$. Incidentally, one can deduce from (3-2) that decaying (or growing) evanescent modes do not carry power,

$$\int_{-\infty}^{\infty} (r_m^{\pm} r_n^{\pm *} - s_m^{\pm} s_n^{\pm *})\, dy = 0 \tag{3-3}$$

The orthogonality relation can be written in a different form since $s^+ = s^{-*}$ and $r^+ = r^{-*}$

$$(\alpha_m - \alpha_n) \int_{-\infty}^{\infty} (r_m^- r_n^- - s_m^- s_n^-)\, dy = 0 \tag{3-4}$$

For m = n, the integral reduces to:

$$(1 - \eta^2) \int_{-\infty}^{\infty} r^2 \, dy \tag{3-5}$$

which is nonzero since η is complex (equation (2-19)). (It is, of course, not necessary to go through the preceding discussion to derive equation (3-4). However, blind manipulation of the coupled-mode equations could lead to frustration. The argument outlined above is helpful and physically appealing.)

3.2 Excitation Coefficients

Assume that an incident surface wave profile U(y) can be expanded as

$$U(y) = \sum_n a_n \bar{r}_n(y) \tag{3-6}$$

The coupled-mode equations impose the simultaneous existence of backward waves

$$S(y) = \sum_n a_n \bar{s}_n(y) \tag{3-7}$$

The expansion coefficient a_n in (3-6) and (3-7) must be the same. Multiplying (3-6) by $\bar{r}_m$ and (3-7) by $\bar{s}_m$ and subtracting the resultant equations, one obtains

$$\sum_n a_n (r_n r_m - s_n s_m) + S s_m = U r_m \tag{3-8}$$

Replacing S by its expansion (3-7) and integrating over all y

$$\sum_n a_n \int_{-\infty}^{\infty} (r_n r_m - s_n s_m) \, dy + \sum_n a_n \int_{-\infty}^{\infty} s_n s_m \, dy = \int_{-\infty}^{\infty} U r_m \, dy \tag{3-9}$$

Applying the orthogonality relation (3-4) leads to a system of linear equations for the excitation coefficients:

$$\begin{bmatrix} \langle r_1^2 \rangle & \langle r_1 r_2 \rangle & \cdots & \langle r_1 r_n \rangle \\ & \langle r_2^2 \rangle & \cdots & \langle r_2 r_n \rangle \\ & & \ddots & \vdots \\ & & & \langle r_n^2 \rangle \end{bmatrix} \begin{bmatrix} a_1 \\ a_2 \\ \vdots \\ a_n \end{bmatrix} = \begin{bmatrix} \langle U r_1 \rangle \\ \vdots \\ \langle U r_n \rangle \end{bmatrix} \qquad (3\text{-}10)$$

$\langle (\cdot) \rangle$ denotes $\int_{-\infty}^{\infty} (\cdot)\, dy$.

The matrix is symmetric (not hermitian). The above formulation is self-consistent. When $U(y) = r_m(y)$ - the IDT is apodized to conform to a given mode-shape - the solution is trivial (but satisfying): $a_m = 1$ and $a_n = 0$ for $n \neq m$, i.e. the other modes are not excited. For wide gratings, the cross terms are negligible,[12]

$$a_n = \frac{\langle U r_n \rangle}{\langle r_n^2 \rangle} \qquad (3\text{-}11)$$

IV. THEORY AND EXPERIMENT

Introduction

The coupling of modes theory is applicable to a variety of grating reflectors. Experimental evidence of transverse modes is available in open and shorted metallic gratings. To account for the experimental observations, appropriate coupling constants are selected. The dispersion relation, mode structure, mode excitation and transducer apodization are then examined using the formalism presented in Chapters II and III.

4.1 Reflection Mechanisms

The choice of reflector in a SAW grating is based on ease of fabrication and tuning as well as on loss and second-order effects inherent to the reflector. In general, one of four reflection mechanisms is exploited:

(a) Topographic reflection[31]

The boundary condition at the discontinuity is the source of the reflected wave. The geometric reflection is employed in the grooved gratings mentioned earlier. The reflectivity of a groove goes to zero linearly in the normalized groove depth (h/λ). Standard fabrication techniques yield reflectivities accurate to less than 0.5 dB. A weighted array can be fabricated by varying the groove depth in the desired manner (RAC devices). The formalism of Chapter II is directly applicable to this reflection mechanism.

(b) Mass loading[33]

A grooved substrate can be visualized as a flat substrate with an overlay. When overlay and substrate have dissimilar density or elastic

constants, a reflection, attributed to "mass loading", occurs. Haus[34] has shown that, in general, mass loading reflection is less effective than topographic reflection. (Mass loaded gratings have other disadvantages with respect to grooved gratings: they are not monolithic and the properties of the overlay are difficult to control.) Alternatively, the properties of the substrate can be altered by ion-implantation or diffusion.[35,36] Experiments suggest that ion-implanted gratings are "fast", which means that, in the coupled-mode description, a non-uniform Rayleigh velocity should be assumed as in (2-10).

(c) Piezoelectric shorting[8,37,38]

Metal strips deposited on a piezoelectric substrate with a large electromechanical coupling constant (K^2), such as Y-Z $LiNbO_3$, periodically short the tangential electric field associated with the piezoelectric Rayleigh wave to produce a reflection commonly referred to as "$\frac{\Delta v}{v}$" reflection. Shorted-strip metal gratings can be treated by the methods of Chapter II.

(d) Electrical regeneration[37,38]

In shorted-strip arrays, piezoelectric shorting is preponderant. In open-strip metal gratings, an additional reflection occurs due to the regeneration of surface waves by the potential induced on a strip. Both types of reflection exist even as the strip thickness goes to zero. Regeneration can be eliminated by breaking up the strips to produce the dot arrays of Solie[39] or the waffle-iron arrays of Matthaei et al.[40]

4.2 The Experiments of Mason et al.[41]

Mason et al. performed experiments on open and shorted metal strip resonators. The distributed mirrors were each 100 wavelengths long, and 20 wavelengths wide, fed by a 9.5 finger pair unapodized IDT.

Amplitude scans of the internal field distribution taken at 8 axial wavelength intervals, using a laser heterodyne point probe, revealed that the open strip acts as a surface waveguide with a discrete set of eigenmodes (Fig. 2). They speculated that the observed modes were the fundamental, the 3rd-order and the 5th-order symmetric modes. The higher-order mode emerges to dominate the field pattern at the end of the mirror. In the case of the shorted grating, only one mode seems to be present with a decay rate that corresponds to $\varkappa_{sc} \approx 1/(34\ \lambda)$. For the open-strip grating, the coupling constant $\varkappa_{oc}$ cannot be deduced as readily from the experimental observations. Instead, an appropriate value of the coupling constant, $\varkappa_{oc} = 1/(26\ \lambda)$, is selected after examining the data available from the theory of gratings of infinite width, from impedance mismatch models, and from optical measurements of the reflection coefficient of a grating.

(a) Optical measurement

The coupling constant $\varkappa$ can be inferred from the experimental results of Cambiaggio et al.[17] Reflectors of 20 Aℓ fingers with a periodicity of 35 μm were constructed on Y-Z $LiNbO_3$. The reflectors were either open or short-circuited. An incident laser beam, many wavelengths wide, is diffracted by the surface displacements which provide a variable phase diffraction grating. The reflection coefficient R is obtained from intensity measurements on the first-order diffracted light (Fig. 4). To relate $\varkappa$ to R, one needs an expression for the reflection coefficient in an infinitely wide grating. It is a simple task to show

$$R = j \frac{\varkappa}{\beta \coth \beta\ell - j\delta} \qquad (4\text{-}1)$$

and since $|R|^2 + |T|^2 = 1$, the transmission coefficient

$$T = \frac{\beta}{\beta \cosh \beta\ell - j\delta \sinh \beta\ell} \qquad (4\text{-}2)$$

where

$\beta = \sqrt{\kappa^2 - \delta^2}$

ℓ = grating length

δ = detuning parameter

Maximum reflection occurs at Bragg ($\delta = 0$)

$$R_{max} = j \tanh (\kappa\ell) \qquad (4\text{-}3)$$

Zero reflection occurs at a detuning δ_{min}

$$\delta_{min} = \sqrt{\kappa^2 + (\frac{n\pi}{\ell})^2}, \qquad n: \text{integer} \neq 0 \qquad (4\text{-}4)$$

The experimental data provides information about δ_{min} and R_{max} from which κ can be deduced through (4-3) or (4-4). A coupling constant $\kappa = 1/(26\ \lambda)$ for open strips and $\kappa = 1/(34\ \lambda)$ for shorted strips provides a good match to the data (Fig. 3).

(b) The theory of metal strip arrays

Bløtekjaer et al.[42] have developed a method to analyze wave propagation in infinitely wide periodic metal strip arrays. The method is based on Legendre polynomial expansions of the electric field when the electromagnetic properties of the structure can be expressed in terms of a wavenumber-dependent permittivity. In the stop-band, the dispersion relation for open and shorted strips with wavenumbers k_{oc} and k_{sc} respectively can be written

$$(k_{\substack{oc\\sc}} - \Lambda)^2 = \frac{(\omega - \omega_1)(\omega - \omega_{2_{\substack{oc\\sc}}})}{v^2} \tag{4-5}$$

where

$$\omega_1 = \frac{\Lambda v}{2}\left[1 - \frac{K^2}{2}(1 - \cos\theta)\right]$$

$$\omega_{2_{\substack{oc\\sc}}} = \frac{\Lambda v}{2}\left[1 - \frac{K^2}{4}\left(1 + \cos\theta \mp \frac{P_{\frac{1}{2}}(\pm\cos\theta)}{P_{-\frac{1}{2}}(\pm\cos\theta)}\right)\right]$$

and

Λ = grating periodicity

v = velocity of propagation

θ = πx (metallization factor) is $\frac{\pi}{2}$ here

$P_{\pm\frac{1}{2}}(\cos\theta)$ = Legendre function of order $\pm\frac{1}{2}$ and argument $\cos\theta$

K^2 = electromechanical coupling constant

In the middle of the stop-band, the reflection coefficient is given by

$$R = j \tanh\left(\frac{\pi}{2} N \frac{\Delta B}{\omega}\right) \tag{4-6}$$

where

N = number of strips

ΔB = normalized stop bandwidth, $\Delta B_{\substack{oc\\sc}} = \mp(\omega_1 - \omega_{2_{\substack{oc\\sc}}})$

The coupling constant $\varkappa$ can be directly related to physical parameters by equations (4-1) and (4-6),

$$\varkappa = \pi \frac{N}{2\ell} \frac{\Delta B}{\omega} \tag{4-7}$$

For a metallization ratio of 0.5, $\Delta B_{oc} = \Delta B_{sc}$. This means that, in an infinitely wide isotropic grating, the coupling constant for

open and short strips has the same magnitude, $|\kappa| \approx \frac{1}{30\lambda}$, intermediate between the values used in the model.

(c) Transmission-line approach

Since the work of Sittig and Coquin,[43] distributed SAW gratings have been modeled as repetitively mismatched transmission lines. The SAW reflector is divided into N sections, each consisting of a quarter wavelength strip of impedance Z_1 and a quarter wavelength gap of impedance Z_o. Because of the impedance discontinuity, each section contributes a small reflection of the surface wave as it propagates. Using a transmission-matrix approach, one can show

$$|R| = \tanh [N\epsilon \sin (\pi t)] \tag{4-8}$$

$$|T| = \operatorname{sech} [N\epsilon \sin (\pi t)] \tag{4-9}$$

where

$$\epsilon = \frac{Z_1}{Z_o} - 1$$

t = fraction of the propagation phase shift that occurs in the perturbed portion of a grating period

Again, the reflection coefficient provides a bridge between the coupled-mode approach and the impedance mismatch approach, but there is a caveat due to an inherent weakness of the impedance mismatch representation. It is not possible to assign unique velocities to the perturbed and unperturbed regions, so that t does not have a simple interpretation, i. e. t is only approximately given by the metallization ratio. Using a phase measurement technique, Cross[37] finds $\epsilon = 0.011 \pm 0.01$ for open strips, while Haydl,[38] using the same technique, gets $\epsilon = 0.0145$. Matthaei[44] deduces $\epsilon = 0.015$ from a transmission measurement through a grating.

Cambiaggio[17] uses $\epsilon = 0.0195$. The discrepancies are partly due to mass-loading effects. The equivalent ϵ in the model is $\epsilon = 0.018$. For shorted strips, the spread in values is much narrower. Cross[37] and Matthaei[44] both find $\epsilon \approx -0.015$, which is equivalent to $\varkappa = 1/(34\,\lambda)$, in agreement with the value deduced from the experimental amplitude scans of Mason et al.[41]

4.3 Coupled-Mode Analysis

The coupling of modes formalism presented in Chapter II is applied to a grating of width $20\,\lambda$ with coupling constant $\varkappa = 1/(26\,\lambda)$. First, the zeros of the dispersion relation (2-23) are determined on a computer using binary search to locate the roots and then linear interpolation in the vicinity of a root. The roots are plotted on a dispersion diagram (Fig. 4) which displays three branches: each one corresponds to a mode. These are the only guided modes of that particular grating reflector. The application of the mode excitation theory of Chapter III with uniform transducer apodization over the width of the grating yields the theoretical amplitude scans of Fig. 5. Although anisotropy and electrical regeneration have been neglected, both the global evolution of the transverse profile and its fine structure at different axial stations are in remarkable agreement with the experimental transverse amplitude scans (Fig. 2). At Bragg, the mode-shape looks "reasonable" (Fig. 6) (observe that the 5-humped mode is the 3rd symmetric mode, not the 5th as conjectured by Mason et al.). The modes have different decay rates; the highest-order mode has the slowest axial decay constant (α) and correspondingly is the less confined transversely. The slow decay explains why the mode eventually emerges to dominate the field pattern at the end of the grating reflector (Figs. 2, 5). It also has the lowest

cut-off frequencies which lead to the passband branch below Bragg and to a leaky mode above.[14] Below Bragg, the mode profile preserves the shape it had at $\delta = 0$. Above Bragg, the mode profile changes pronouncedly (Fig. 7). No obvious trait is available to identify a particular mode, such as preservation either of the envelope or of the number of wiggles. The metamorphosis of mode profile is more rapid the closer a mode is to its cut-off frequency, the modes that are relatively far from their cut-off being unaffected (compare Figs. 8 and 9).

4.4 Apodization

Experimental evidence suggests two methods to suppress transverse modes:

(a) Decrease the width of the grating (which is not always practical). This is a consequence of the dispersion relation; Wang[14] has shown that the n^{th} symmetric mode cuts off when

$$(n - 1) = \frac{2w}{\sqrt{m\pi}} \qquad (4\text{-}10)$$

which also reveals the dependence of the number of guided modes on the coupling constant ($\varkappa = 1/(m\lambda)$).

(b) Tailor the IDT apodization to conform to the fundamental grating mode. Typical weightings are cos, $\cos^2$ and gaussian. The cosine shape conforms very closely to the fundamental mode amplitude (Fig. 10), which, in light of the discussion of mode excitation in Chapter II, shows why it is so effective. Even when the apodization conforms closely to the fundamental mode profile, higher-order modes are excited and, since they have the lower decay rates, eventually dominate the field pattern.

However, the amplitudes are so low by then (down by factors of 10^3), that this effect is negligible (Figs. 11, 12).

It is possible, in principle at least, to find the "point source" response of a grating (Fig. 13), but the concept is of little usefulness since the grating does not satisfy translational invariance in the transverse direction.

When a grating is wide enough ($w >> \lambda$) or has a coupling constant which is large enough, the modes are tightly bound to the grating with negligible energy outside, viz.

$$R(y) \approx \cos a_1 y - \frac{\cos a_1 w}{\cosh a_2 w} \cosh a_2 y \qquad (4\text{-}11)$$

An expansion into these modes is easy since they are orthogonal. In the case at hand, too much energy is still outside the grating since the transverse amplitude scan using the approximate modes (Fig. 14) is different from the one obtained using the exact modes (Fig. 5). For shorted gratings, there is, as mentioned earlier, general agreement that the appropriate coupling constant is $\kappa_{sc} = 1/(34\,\lambda)$. The coupling of mode formalism applied to a grating width of 20 λ yields two modes. The fundamental mode is apparently the only one present or excited in the experiment of Mason et al.[41] That fact cannot be accounted for by assuming a non-uniform Rayleigh velocity ($\frac{\Delta v}{v}$ type guidance). Anisotropy in Y-Z $LiNbO_3$ tends to increase the effective width of the grating, which could alter the relative excitation of the two modes. It is evident from the discussion on apodization that the effective width of the transducer could also play an important role in the relative excitation of grating modes. A measure of relative excitation is the ratio of excitation coefficients $|a_1/a_2|$ (Fig. 15). In particular, a uniformly apodized

transducer, 13.2 λ wide, would not, for all practical purposes, excite the second mode.

The mode excitation formulation can quite easily accommodate a large number of modes (the excitation matrix is symmetric and thus efficiently invertible, while the apodization integrals can be computed using a Romberg integration scheme). A typical grating has an aperture of 50 λ. For a coupling constant $\varkappa = 1/(26\ \lambda)$, it would support six modes. Figure 16 shows an amplitude scan at the aperture when the incident surface wave has uniform apodization.

CONCLUSION

The theory of mode excitation in SAW grating reflectors of finite width has helped unravel the mode structure of an open-strip metal grating. As for the shorted grating, it is believed that some mechanism (anisotropy or other) is altering the relative excitation of the modes to produce the observed experimental results. The theory of mode excitation leads to a very simple treatment of apodization which could be of interest in the design of SAW devices. In particular, if uniform apodization were desired, the theory would predict the optimal IDT width which would minimize the excitation of higher order modes.

Electrical regeneration - whereby the potential induced on a strip by an incident surface wave in turn gives rise to a reflected surface wave - has been neglected. It is suggested that electrical regeneration, negligible in shorted gratings and apparently not important in the open-strip grating examined here, should be studied to achieve a better understanding of multistrip coupler behavior in the stop-band. It is a global effect and can be incorporated into the coupled-mode formalism through the addition of appropriate integral terms.

LIST OF FIGURES

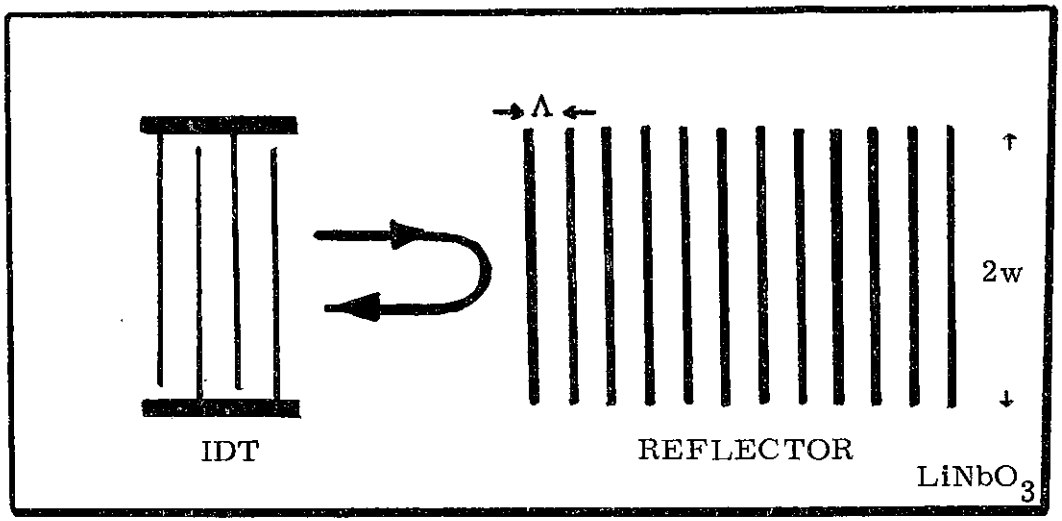

Fig. 1 Open-strip metallic grating reflector.

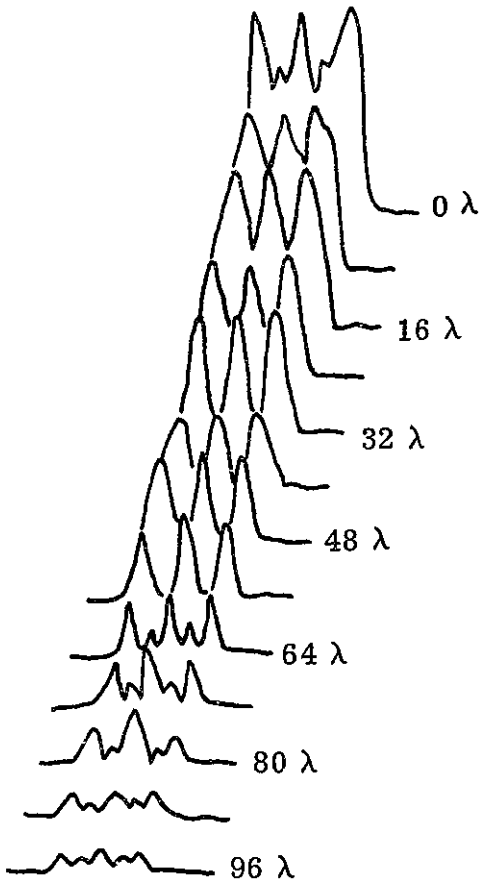

Fig. 2 Transverse amplitude scan.

[Experiment, Mason et al.]

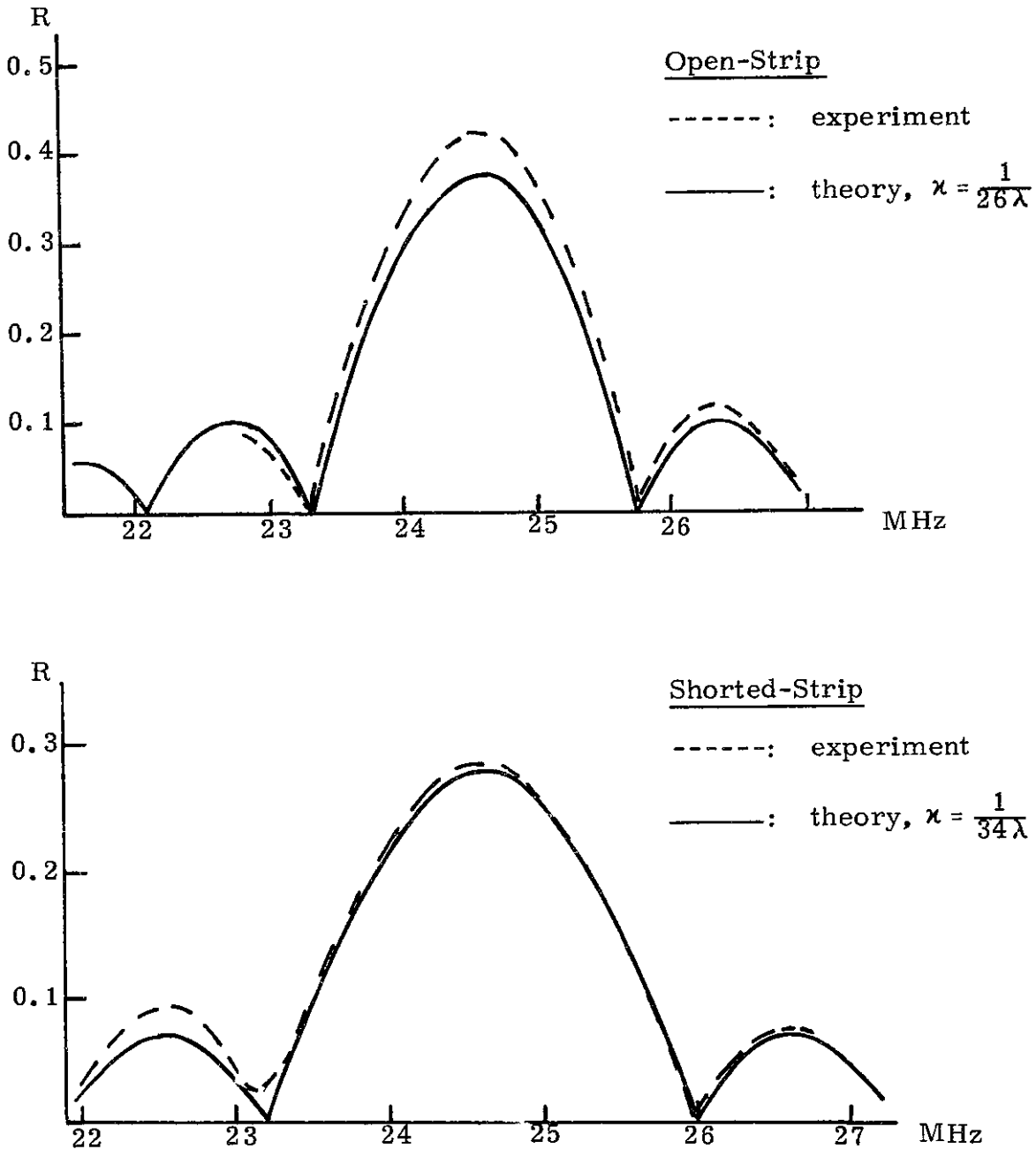

Fig. 3 Reflection coefficient for open and shorted strip metal gratings. [Experiment, Cambiaggio et al.]

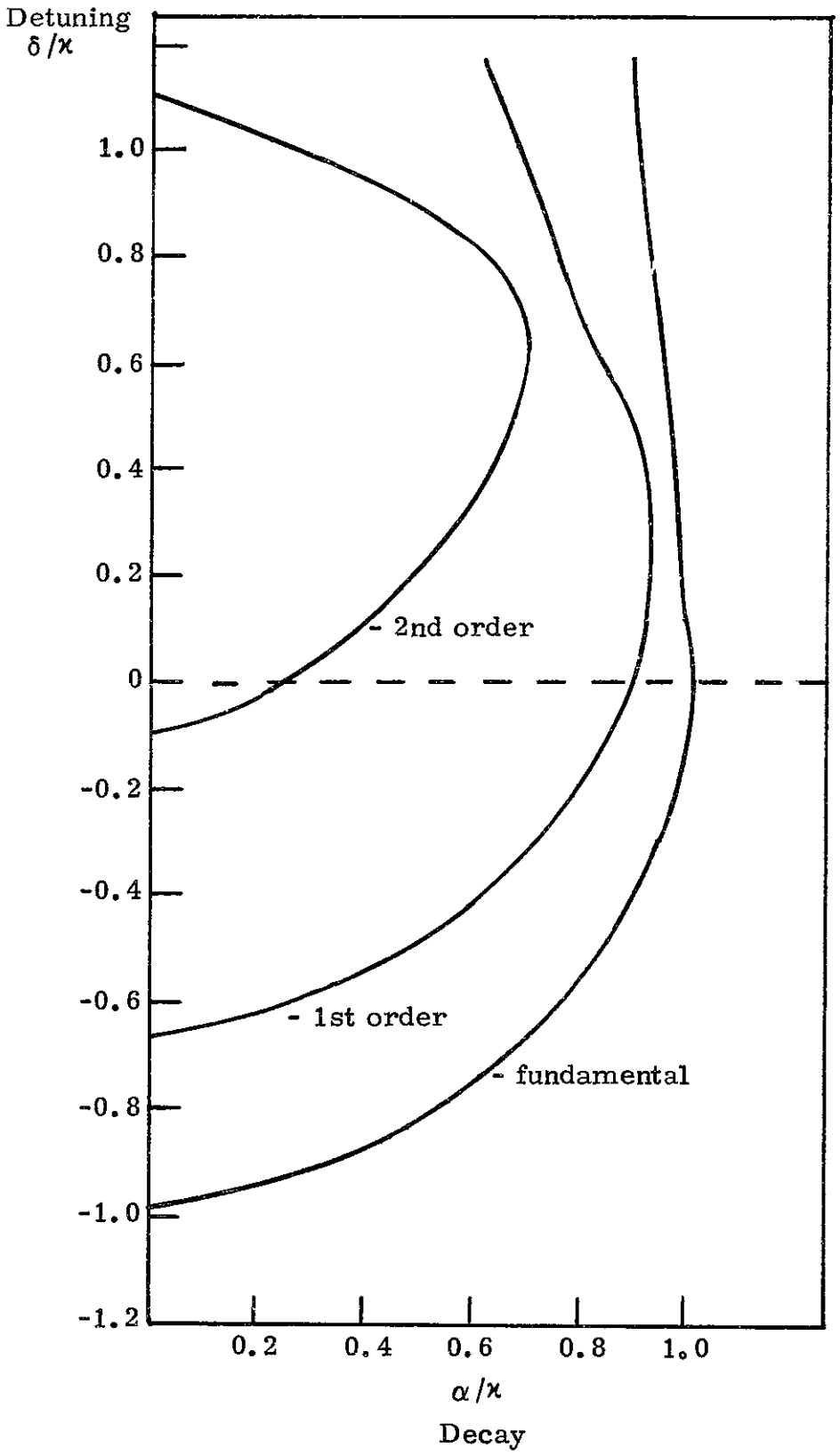

Fig. 4 Dispersion diagram.

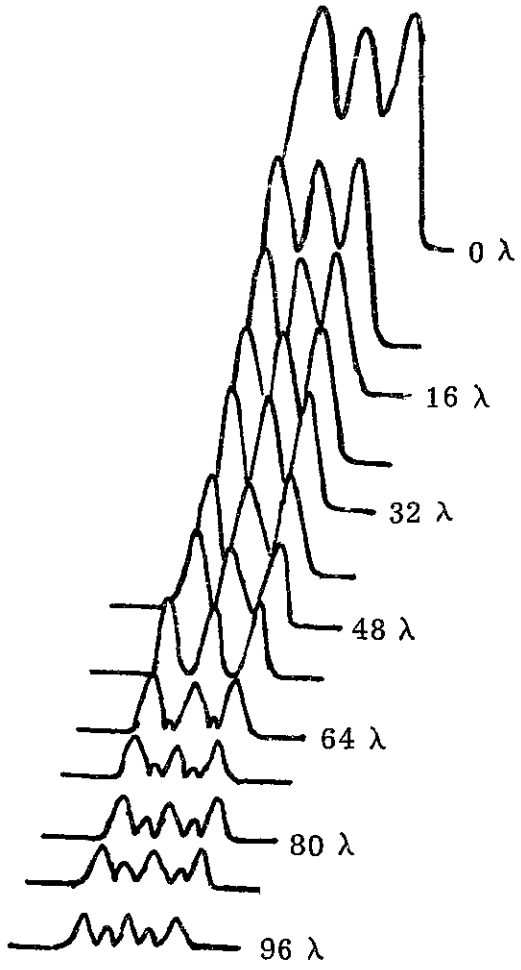

Fig. 5 Transverse amplitude scan (theory).

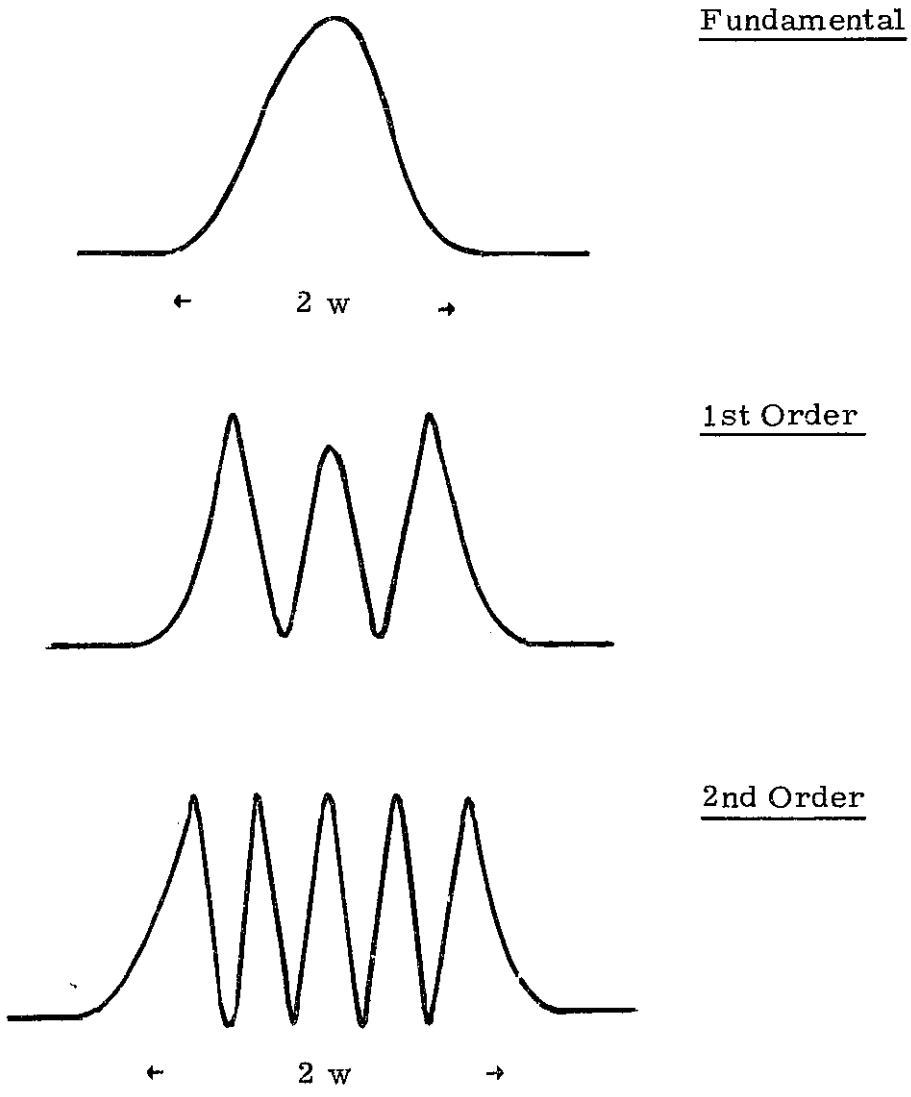

Fig. 6 Grating modes at Bragg.

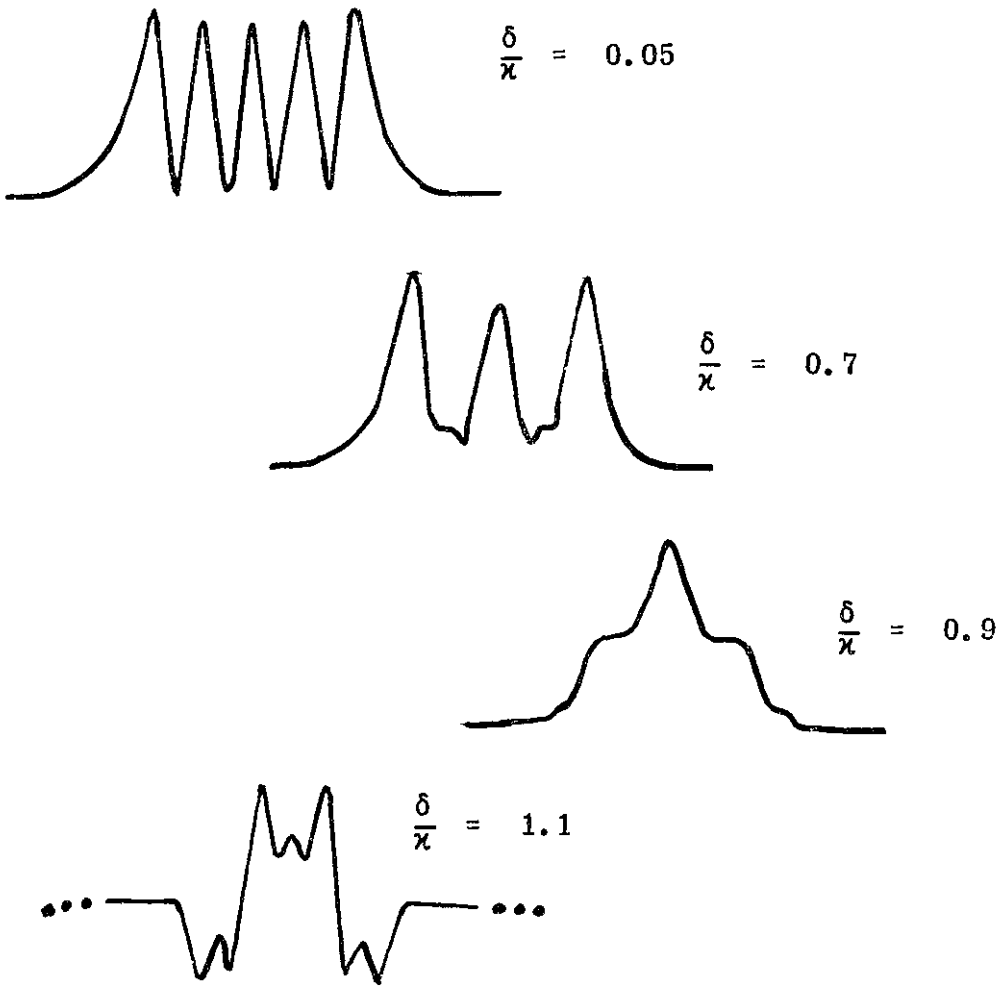

Fig. 7 Metamorphosis of the highest order mode with increasing detuning.

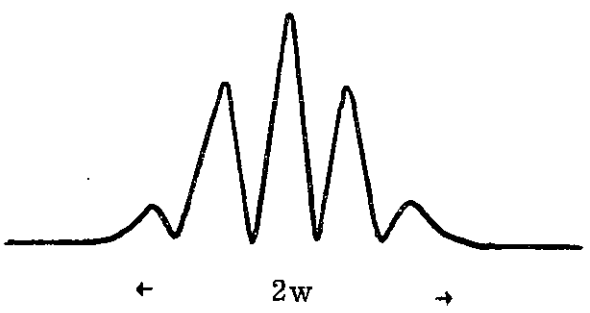

Fig. 8 Grating modes at $\delta/\varkappa = 1.0$.

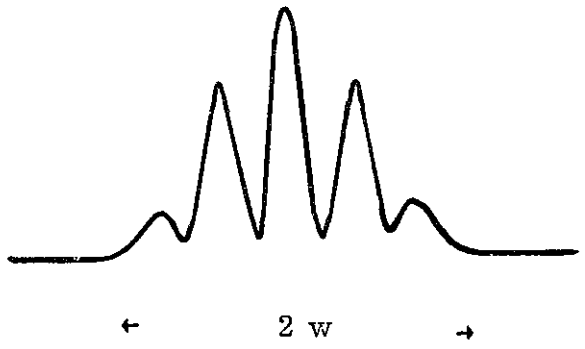

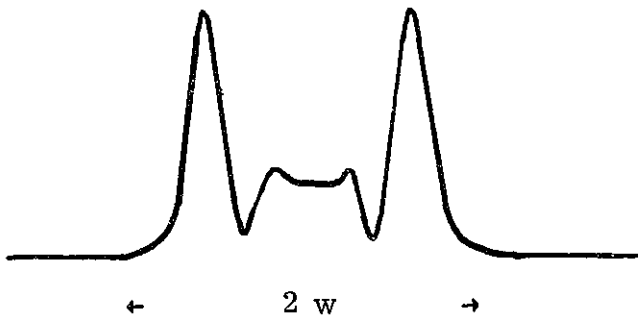

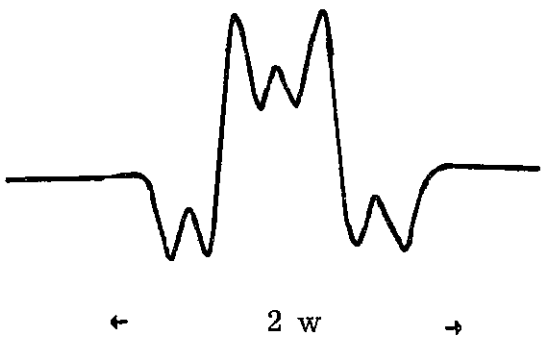

Fig. 9 Grating modes at $\delta/\varkappa = 1.1$.

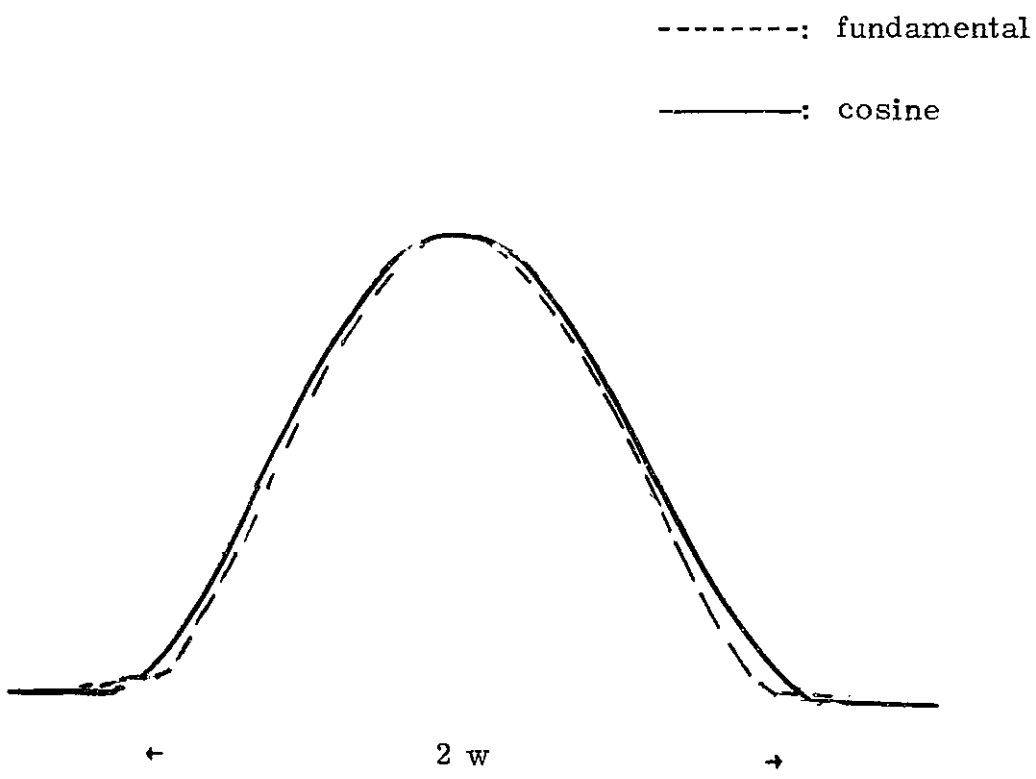

Fig. 10 Intensity of fundamental mode compared with $\cos^2 (\frac{\pi y}{2w})$.

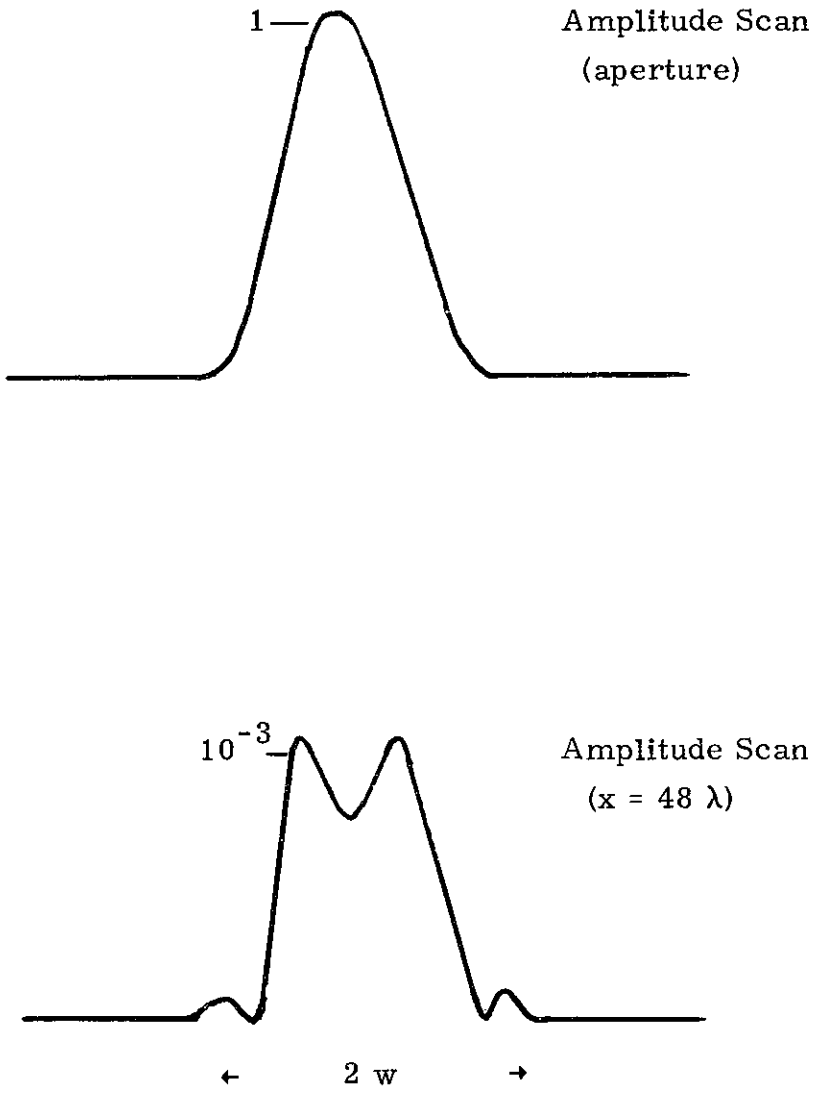

Fig. 11 Apodization: magnitude of fundamental for $|y| \leq 0.5$ w.

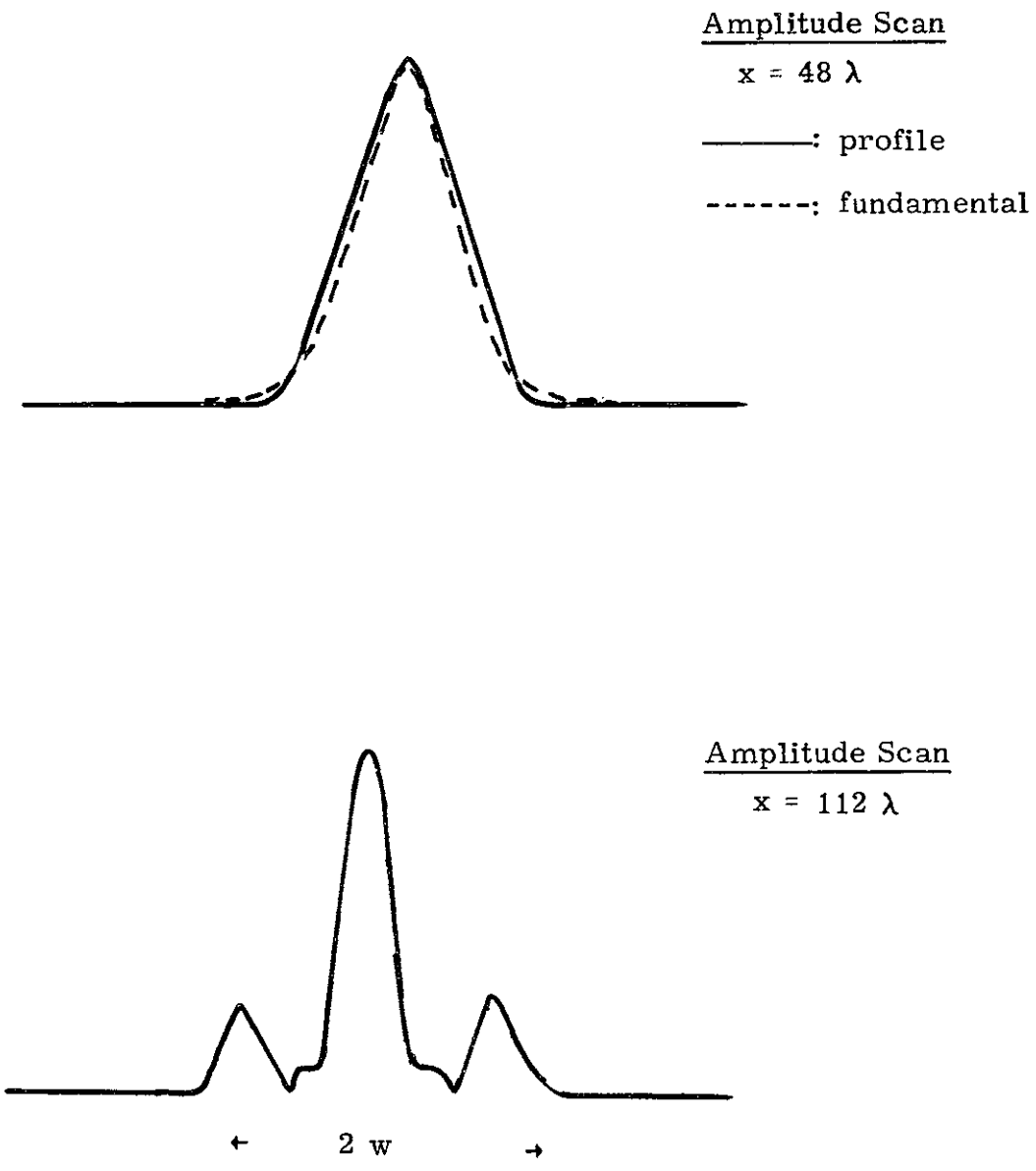

Fig. 12 Apodization: magnitude of fundamental for $|y| \leq 10$ w.

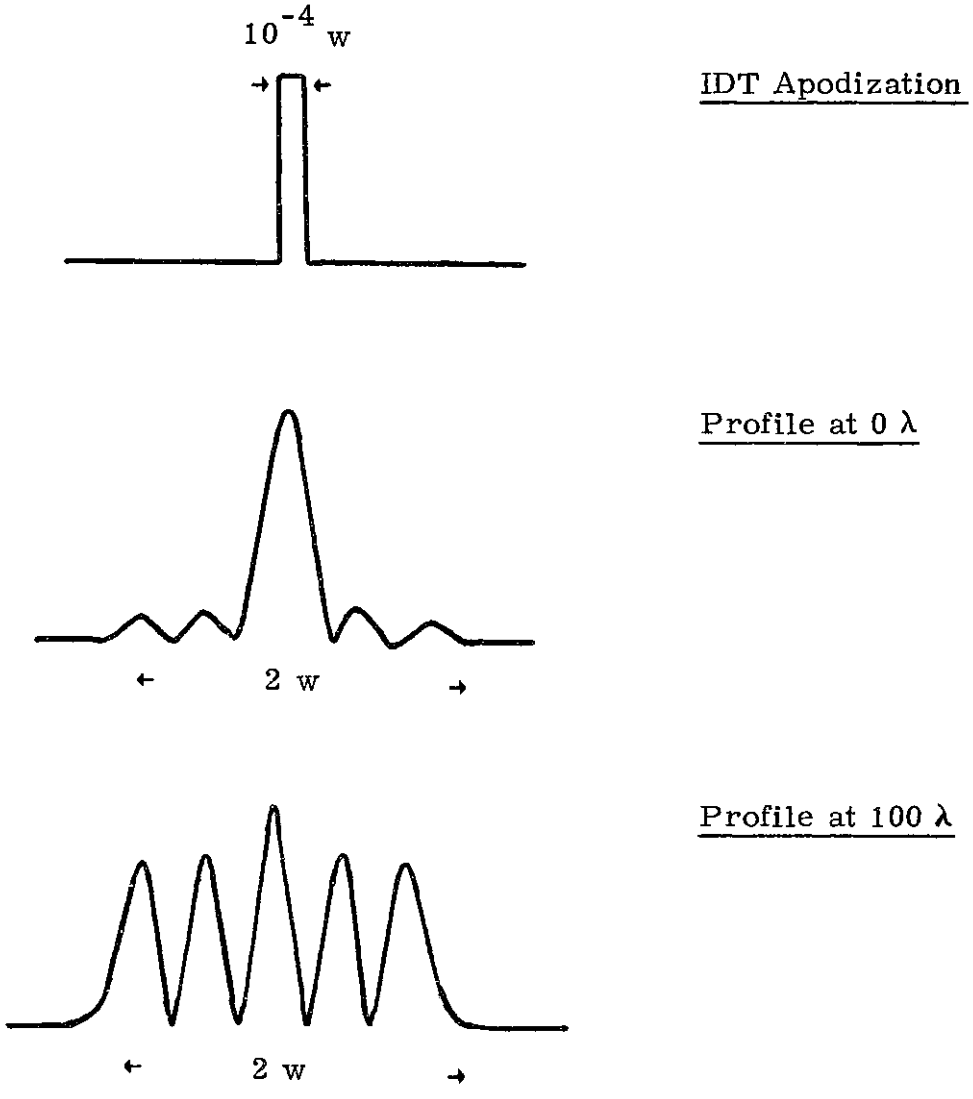

Fig. 13 "Point source" response (Bragg).

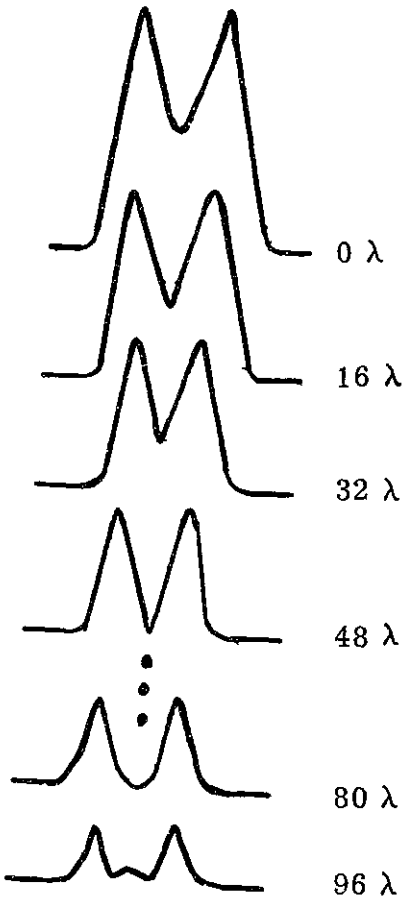

Fig. 14 Transverse amplitude scan (approximate modes).

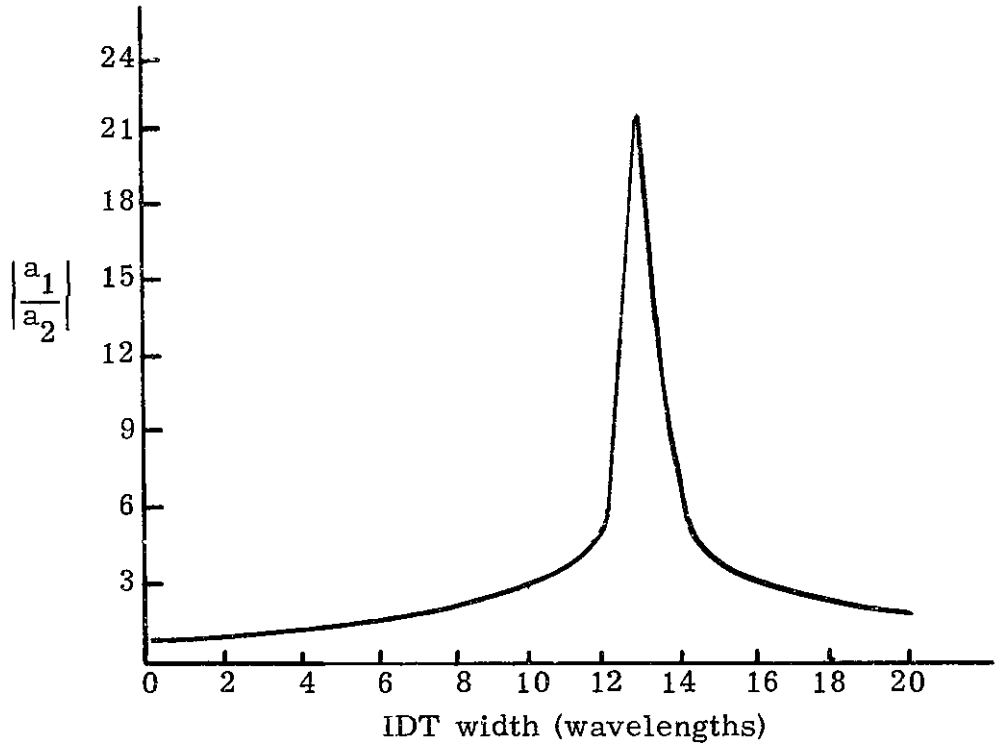

Fig. 15 Magnitude of the ratio of excitation coefficients of fundamental and 1st order mode as the width of an IDT with uniform apodization changes. [Grating width: 20 λ, $\varkappa = 1/(34\ \lambda.]$

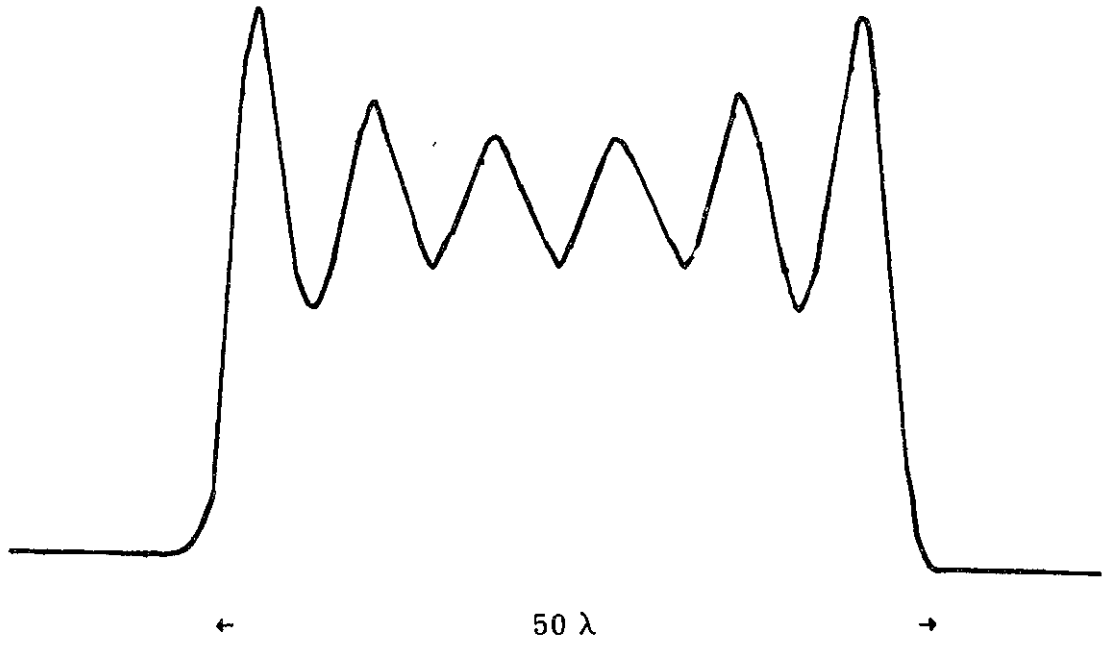

Fig. 16 Transverse amplitude scan (aperture).

[Grating width: 50 λ, $\varkappa = 1/(26\ \lambda)$.]

BIBLIOGRAPHY

1. H. Kolsky, "Stress Waves in Solids", Dover Publications, New York, 1963.

2. R. M. White, "Surface Elastic Waves", Proc. IEEE, Vol. 58, No. 8, pp 1238-1276, August 1970.

3. A. J. Slobodnik, Jr., "Surface Acoustic Waves and SAW Materials", Proc. IEEE, Vol. 64, No. 5, (581), May 1976.

4. R. M. White and F. W. Voltmer, "Direct Piezoelectric Coupling to Surface Acoustic Waves", Appl. Phys. Letters, Vol. 7, pp 314-316, December 1965.

5. A. Slobodnik, T. Szabo, and K. Laker, "Miniature Surface-Acoustic-Wave Filters", Proc. IEEE, Vol. 67, No. 1, January 1979.

6. H. A. Haus, "Two-Dimensional Rayleigh Waves", Electrodynamics Memo No. 57, July 1976.

7. E. A. Ash, "Surface Wave Grating Reflectors and Resonators", (Abstract only), 1970 IEEE Symposium on Microwave Theory and Techniques, Symposium Digest (395), 1970.

8. E. J. Staples, "UHF SAW Resonators", Proc. 28th Annual Frequency Control Symposium, pp 280-285, May 1974.

9. W. J. Tanski and H. Van de Vaart, "The Design of SAW Resonators on Quartz with Emphasis on Two Ports", 1976 Ultrasonics Symposium, IEEE Cat. #76 CH 1120-5SU, 260-265.

10. R. C. Li, J. A. Alusow, and R. C. Williamson, "Experimental Exploration of the Limits of Achievable Q of Grooved Surface Wave Resonators", 1975 Ultrasonics Symposium, IEEE Cat. #75 CH 0994-4SU, pp. 279-283.

11. E. J. Staples and R. C. Smythe, "Surface Acoustic Wave Resonators on ST-quartz", 1975 Ultrasonics Symposium, Cat. #75 CH 0994-4SU, pp 307-310.

12. H. A. Haus, "Modes in SAW Grating Resonators", J. Appl. Phys. 48, No. 12, pp 4955-4961 (December 1977).

13. H. A. Haus and K. L. Wang, "Modes of Grating Waveguide", J. Appl. Phys. 49, No. 3, pp 1061-1069 (March 1978).

14. K. L. Wang, Ph.D. dissertation (MIT, 1978), unpublished.

15. E. Cambiaggio and F. Cuozzo, "Surface Acoustic Wave Scattering

from Metallic Strips Deposited on the Surface of a $LiNbO_3$ Crystal", 1975 Ultrasonics Symposium, Proc. IEEE, Cat. #75 CH 0994-4SU, pp 444-446.

16. E. Cambiaggio, F. Cuozzo, and E. Rivier, "Finite Difference Analysis of Piezoelectric Surface Wave Behavior on Surface Discontinuities ...", 1976 Ultrasonics Symposium, Proc. IEEE, Cat. #76 CH 1120-5SU.

17. E. Cambiaggio, F. Azan, and A. Lantz, "SAW Refection from Metallic Gratings of Periodicity λ and Applications to Resonators", 1978 Ultrasonics Symposium, Proc. IEEE Cat. #78 CH 1344-1SU, pp 643-646.

18. J. Knowles, "A Note on Elastic Surface Waves", Jour. Geophysical Res., Vol. 71, No. 22, pp 5840-5841, 1966.

19. M. Cohen, "Optical Study of Ultrasonic Diffraction and Focusing in Anisotropic Media", J. Appl. Phys. Vol. 38, No. 10, pp 3821-3828, 1967.

20. T. L. Szabo and A. J. Slobodnik, Jr., "The Effect of Diffraction on teh Design of Acoustic Surface Wave Devices", IEEE Trans. Sonics Ultrason., SU-20, pp 240-251, 1973.

21. T. L. Szabo and A. J. Slobodnik, Jr., "Diffraction Compensation in Periodic Apodized Acoustic Surface Wave Filters", IEEE Trans. Sonics Ultrason., SU-21, pp 114-119, 1974.

22. L. A. Coldren, H. A. Haus, and K. L. Wang, "Experimental Verification of Mode Shape in SAW Grating Resonators", Electron. Lett. 21, 642-644, 1977.

23. I. Mason and E. Ash, "Acoustic Surface-Wave Beam Diffraction on Anisotropic Substrates", J. Appl. Phys. Vol. 42, No. 13, pp 5343-5351, 1971.

24. C. Elachi, "Waves in Active and Passive Periodic Structures", Proc. IEEE, Vol. 64, No. 12, p 1666, 1976.

25. A. Yariv and A. Gover, "Equivalence of the Coupled-Mode and Floquet-Mode Formalisms in Periodic Optical Waveguides", Appl. Phys. Lett., Vol. 26, No. 9, pp 537-539, 1975.

26. J. R. Pierce, "Coupling of Modes and Propagation", J. Appl. Phys. Vol. 25, No. 2, 179-183, 1954.

27. J. R. Pierce, Almost All About Waves (MIT Press, Cambridge, 1967).

28. A. Yariv, "Coupled Mode Theory for Guided-Wave Optics", IEEE J. Quant. Electron. QE-9, No. 9, pp 919-933, 1973.

29. H. Kogelnik and C. V. Shank, "Coupled-Wave Theory of Distributed Feedback Lasers", J. Appl. Phys. Vol. 43, No. 5, (2327), 1972.

30. H. A. Haus, "Grating-Filter Transformation Chart", Electron. Lett. 11, No. 23, pp 453-454, 1975.

31. R. C. M. Li, J. Melngailis, "The Influence of Stored Energy at Step Discontinuities on the Behavior of Surface-Wave Gratings", IEEE Trans. Sonics and Ultrason., SU-22, No. 3, pp 189-198, 1975.

32. D. Lee, Ph.D. Thesis (MIT, 1977), unpublished.

33. E. J. Staples, J. S. Schoenwald, R. C. Rosenfeld, and C. S. Hartmann, "UHF Surface Acoustic Wave Resonators", 1974, Ultras. Symp. Proc. IEEE Cat. #74, CH 0896-1SU, pp 263-267.

34. H. A. Haus, "Bulk Scattering Loss of SAW Grating Cascades", IEEE Trans. SU-24, No. 4, pp 259-267, 1977.

35. P. Hartemann, "Ion Implanted Acoustic-Surface Wave Resonator", Appl. Phys. Lett. Vol. 28, #2, pp 73-75, 1976.

36. P. Hartemann, "SAW Guidance Produced by Ion Implantation in Quartz", Electr. Lett., Vol. 10, #7, pp 110-111, 1974.

37. P. S. Cross, "Properties of Reflective Arrays for Surface Acoustic Resonators", IEEE Trans. SU-23, #4, pp 255-262, 1976.

38. W. H. Haydl, B. Dishler, and P. Hiesinger, "Multimode SAW Resonators - A Method to Study the Optimum Resonator Design", 1976 Ultras. Symp. Proc., IEEE Cat. #76, CH 1120-5SU, pp 287-296.

39. L. P. Solie, "A SAW Filter Using a Reflective Dot Array (RDA)", IEEE 1976 Ultras. Symp. Proc., Cat. No. 76, CHO 1120-5SU, pp 309-312.

40. G. L. Matthaei, F. Barman, "Study of the Q and Modes of SAW Resonators Using Metal 'Waffle-Iron' and Strip Arrays", IEEE Trans. Sonics Ultras. SU-25, No. 3, pp 138-146, 1978.

41. I. M. Mason, J. Chambers, and P. E. Lagasse, "Laser Probe Analysis of Field Distributions Within Acoustic Surface-Wave Resonators", Electr. Lett., Vol. 11, No. 14, 288-290, 1975.

42. K. Bløtekjoer, K. Ingebrigtsen, and H. Skeie, "A Method for Analyzing Waves in Structures Consisting of Metal Strips on Dispersive Media", IEEE Trans. ED-20, No. 12, 1133-1138, 1973. Also, same issue, "Acoustic Surface Waves in Piezoelectric Materials with Periodic Metal Strips on the Surface", 1139-1146.

43. E. K. Sittig and G. A. Coquin, "Filters and Dispersive Delay Lines Using Repetitively Mismatched Ultrasonic Transmission Lines", IEEE Trans., SU-15, 111-119, 1968.

44. G. L. Matthaei, F. Barman, E. B. Savage, "SAW Reflecting Arrays", Elect. Lett., Vol. 12, No.21, 556-557, 1976.